PROCEEDINGS OF SPIE

SPIEDigitalLibrary.org/conference-proceedings-of-spie

# Classification of brain injury severity using a hybrid broadband NIRS and DCS instrument with a machine learning approach

Danai Bili, Frédéric Lange, Kelly Harvey Jones, Veronika Parfentyeva, Turgut Durduran, et al.

Danai Bili, Frédéric Lange, Kelly Harvey Jones, Veronika Parfentyeva, Turgut Durduran, Nikki Robertson, Subhabrata Mitra, Ilias Tachtsidis, "Classification of brain injury severity using a hybrid broadband NIRS and DCS instrument with a machine learning approach," Proc. SPIE 12628, Diffuse Optical Spectroscopy and Imaging IX, 126280D (9 August 2023); doi: 10.1117/12.2670657

SPIE.

Event: European Conferences on Biomedical Optics, 2023, Munich, Germany

# Classification of Brain Injury Severity Using a Hybrid broadband NIRS and DCS Instrument with a Machine Learning Approach

Danai Bili*[a], Frédéric Lange[a], Kelly Harvey Jones[b], Veronika Parfentyeva[c], Turgut Durduran[d], Nikki Robertson[b], Subhabrata Mitra[b], Ilias Tachtsidis[a]

[a] Department of Medical Physics and Biomedical Engineering, University College London, Malet Place, London, WC1E 6BT, United Kingdom
[b] Neonatology, Institute for Women's Health, University College London, London, WC1E6HU, United Kingdom
[c] Institucio Catalana de Recerca i Estudis Avançats (ICREA), Carrer de la Dispatio, Barcelona, 08015, Spain
[d] eICFO-Institut de Ci'encies Fot'oniques, The Barcelona Institute of Science and Technology, Castelldefels, Barcelona, 08015, Spain

*danaibili2@gmail.com

## ABSTRACT

Optical biomarkers of neonatal hypoxic ischemic (HI) brain injury can offer the advantage of continuous, cot-side assessment of the degree of injury; research thus far has focused on examining different optical measured brain physiological signals and feature combinations to achieve this. To maximize the breadth of physiological characteristics being taken into consideration, a multimodal optical platform has been developed, allowing unique physiological insights into brain injury. In this paper we present an assessment of severity of injury using a state-of-the-art hybrid broadband Near Infrared Spectrometer (bNIRS) and Diffusion Correlation Spectrometer (DCS) instrument called FLORENCE with a machine learning pipeline. We demonstrate in the preclinical neonatal model (the newborn piglet) that our approach can identify different HI insult severity (controls, mild, severe). We show that a machine learning pipeline based on k-means clustering can be used to differentiate between the controls and the HI piglets with an accuracy of 78%, the mild severity insult piglets from the severe insult piglets with an accuracy of 90% and can also differentiate the 3 piglet groups with an accuracy of 80%. So, this analytics pipeline demonstrates how optical data from multiple instruments can be processed towards markers of brain health.

**Keywords:** HIE, NIRS, DCS, Machine Learning, Clustering, Biomarkers

## 1. INTRODUCTION

Neonatal hypoxic ischemic encephalopathy (HIE) is caused by the lack of adequate oxygen and blood flow in the brain of the newborn infants[1]. HIE affects 2-3 in 1000 live births in high income countries, and manifests from the first hours of life [1,2] Pathophysiological changes following hypoxic ischaemic (HI) injury in newborn brain evolves over time, starting with a primary cellular energy failure, followed by a latent phase that lends itself as a treatment window, a third phase which is a secondary cellular energy failure and ultimately the tertiary phase lasting for months to years leading to further deranged function[4]. Proton Magnetic Resonance Spectroscopy ($^1$H MRS) quantification of cerebral metabolism in the form of deep grey matter (DGM) Lactate/NAA ratio (Lac/NAA) has been shown to be an accurate predictor of neurodevelopmental outcome[3].

The protocol of HIE treatment in the clinic is focused on the placement of the infant under therapeutic hypothermia for infants with moderate and severe encephalopathy. This treatment reduces the body temperature to 33.5 degrees Celsius and is maintained for 72 hours before bringing the temperature gradually back to normal. This process

Diffuse Optical Spectroscopy and Imaging IX, edited by Davide Contini, Yoko Hoshi, Thomas D. O'Sullivan, Proc. of SPIE Vol. 12628, 126280D

allows the metabolic rate to slow down and reduce the neuroinflammatory cascade of reactions, modulating the severity of the insult[2]. To date, there has been an extensive hunt for biomarkers of HIE using optical technologies and in particular near-infrared spectroscopy (NIRS) techniques[5]. So far, these biomarkers were focused on either cerebral oximetry using multidistance NIRS or broadband NIRS (bNIRS) or diffuse correlation spectroscopy (DCS)[6]. bNIRS brain tissue measurements of the oxidation state of Cytochrome - c – oxidase (oxCCO) have shown that it can reveal information on brain injury severity[7,8,9]. In this study, we present an assessment of the severity of HIE using optical data captured by FLORENCE, an integrated hybrid broadband near infrared spectrometer (bNIRS) and diffusion correlation spectrometer (DCS) instrument and a machine learning pipeline based on k-means clustering for classification. We demonstrate the approach in the neonatal preclinical model, the newborn piglet, following different levels of HI insults.

## 2. HARDWARE

FLORENCE is an in-house developed hybrid bNIRS-DCS instrument. . The bNIRS consists of a tungsten halogen lamp light source (HL-2000-FHSA, Ocean Optics, USA) with a 700nm longpass filter, and a custom-made micro spectrometer (644-917nm, cooled CCD, 1024 pixels, Wasatch Photonics, USA). The DCS system (custom-made by Hemophotonics), consists of a 785nm long coherence (>8m) diode laser and a 4-channel APD detector. To guide the light to the piglet, a multimode fibre (400 μm, 0.37NA) is used for the DCS laser, and a fibre bundle of 2.5 mm (30μm fibres, 0.55 NA) is used for the bNIRS halogen source. For the detection, a single fibre bundle is used to direct the light to the 4 APDs (4 single mode fibres, 3.5μm, 0.13 NA) for the DCS, and to bNIRS (2 mm bundle of 30μm fibres, 0.55 NA). All the fibres were made by Fiberoptic Sytems, USA and were 3 meters long. A custom 3D printed probe holder was designed to securely attach the fibres on the head of the piglet; with a source-detector separation of 3cm and 2cm for the bNIRS and the DCS respectively. We use computer-controlled shutters to time multiplex the two instruments, allowing fast sequential measurements from each modality. The FLORENCE measurements (typical recording lasts for more than 1 hour) include the changes in concentration of oxy- and deoxy-haemoglobin ($HbO_2$, HHb) from which we can derive brain oxygenation changes (HbDiff, HbD=$HbO_2$-HHb) and brain blood volume changes (HbT=$HbO_2$+HHb); the changes in the oxidation state of cytochrome-c-oxidase (oxCCO), calculated from the modified beer-lambert law[10]; and the cerebral blood flow index (BFi). Note that we use the broadband fitting method to estimate the absorption and scattering coefficient of the tissue in order to inform the BFi calculation[10].

## 3. PROTOCOL

Newborn white male piglets aged ≤36h were sedated with intramuscular midazolam (150μg) and anaesthetized with 2-3% v/v isoflurane. Following this umbilical arterial and venous catheters were inserted for continuous monitoring of systemic physiology and inflatable occluders were placed around both common carotid arteries. This study was conducted in accordance with the UK Home Office Guidelines [Animals (Scientific procedures) Act, 1986] and complies with ARRIVE guidelines. The Ethics Committee of University College London approved the study. The probes of the FLORENCE system were then securely placed on top of the piglet head. Following a short baseline period (10 min), we induced a transient HI by remote occlusion of both common-carotid arteries, and with simultaneous reduction of fractional inspired oxygen ($FiO_2$) in steps down to 6-9%. The HI period was adjusted to either 20min for a mild injury (n=6) or 25min for a severe injury (n=7). Following the HI period, occluders were deflated and $FiO_2$ was normalised (recovery period). In addition, we included a control group (n=6) that did not experience HI. For a duration of 6 hours, the piglets underwent a period of monitoring, and following that, an $^1$H MRS was performed. From the $^1$H MRS, the Lac/NAA ratio was derived for each piglet.

## 4. METHOD

### 4.1 Data Pre-Processing and Feature Extraction

The bNIRS raw data was denoised by being filtered for outliers in the frequency space, and fitted using the UCLn algorithm, to extract the relative changes in concentration of the $HbO_2$, HHb, oxCCO. The fitted bNIRS and BFi signals were passed through a z transform.

Table I

| Feature Extracted | Process |
|---|---|
| Peak Value (Peak Val) | Total signal maximum value. |
| Area Under Curve (AUC) | Area Under Curve of insult normalized by its duration. |
| Time of Insult (Peak Loc) | Time point of insult. |
| Insult Average (Ins Avg) | The average value of the insult. |
| Baseline Average (Bas Avg) | The average value of the signal for 500s before the insult. |
| After Insult Average (Aft Ins Avg) | The average value of the signal for 500s after the insult. |

Table I. A table detailing the method by which each extracted feature was captured.

Piglets with no insult were assigned NANs to the corresponding features. The datasets present included features that had been captured in the z-space, by taking the z – transformation of the processed signal, and features that had been derived by performing a transformation starting from the z space and mapping to the relative power (rpwr) and relative cost (rcst) space. The latter was considered in order to quantify the coupling between chromophores, and was given by:

$$\begin{bmatrix} rPWR \\ rCST \end{bmatrix} = \begin{bmatrix} \cos(45^\circ) & \sin(45^\circ) \\ -\sin(45^\circ) & \cos(45^\circ) \end{bmatrix} \begin{bmatrix} z(\text{ signal 1}) \\ z(\text{ signal 2}) \end{bmatrix} \quad (1)$$

Where the two signals, signal 1 and signal 2, correspond to the signals of each chromophore in the couple that is being examined[11]. In this 2 dimensional space, the operation in (1) describes a rotation of the axes by 45 degrees. For a system of two quantities, as projected on the 2 dimensional space, this rotation of the axes allows us to quantify how strongly the two quantities match for the case of rpwr and how strongly two quantities are exhibiting a mismatch[11]. So, this way we were able to include the coupling between features in our analysis. The features from the 2 spaces, z space and *rpwr-rcs*t space, were treated as independent and the analysis was repeated separately for the two sets of features. This was due to the strong dependence between the values themselves in the z space and their rotation in the *rpwr-rcst* space which would result in intercorrelations that would in turn lead to the representation of the same underlying mechanism multiple times.

### 4.2 Machine Learning Pipeline and Biomarker Identification

The analysis was split into 3 scenarios: the first, case 1, being mild vs severe cases, the second, case 2, being HIE vs controls and the third, case 3, being controls vs mild vs severe cases. Figure 4.1 shows a flowchart of the processing pipeline. The datasets of z space and *rpwr-rcst* space features were propagated through the developed machine learning pipeline, which consisted of feature selection to visually inspect the significance of the features, dimensionality reduction to move from the 6-dimensional feature space into a 2-dimnsional space, moving to a configuration in which features are examined as a linear superposition projected onto 2 orthogonal axes, and a k-means clustering algorithm. The principal component analysis allowed us to visually inspect the output of the clustering classification step.


Fig.4.1. The pipeline that was developed in order to process and recognize groups of hypoxic ischemic severity in the piglet dataset.

The clustering required the definition of the number of groups to be searched for. Case 1 and case 2 were assigned k=2 in the clustering, while for case 3 a k=3 clustering algorithm was applied. The decision boundaries were drawn in the 2-dimensional space, and were given by a support vector machine radial basis function, defined as:

$$K(X_1, X_2) = \exp\left(-\gamma \|X_1 - X_2\|^2\right) \quad (2)$$

with $\|X1\text{-}X2\|^2$ being the squared Euclidean distance between the points and γ a regularization parameter. In order to gauge the accuracy of the pipeline, the Rand Index was applied. The metric chosen was given by:

$$\mathrm{RI} = \frac{a+b}{C_2^{n_{\text{samples}}}} \quad (3)$$

with α being the number of true positives and true negatives, $b$ the number of false positives and false negatives, and $C_2^{n_{\text{samples}}}$ the total number of pairs that can exist in the dataset.

## 5. RESULTS

The classification of piglets based on each feature extracted, for all chromophores and BFi, was successful in identifying the groups of piglets that had undergone the same degree of hypoxic ischemic injury. This was found to be the case in all 3 cases considered. This allowed the assessment of the performance of the pipeline when undertaking different tasks, such as the recognition of a group of controls or the identification of 3 separate groups of hypoxic ischemic injury prevalence, as well as the gauging of biomarkers to be used as accuracy enhancing features of a machine learning pipeline. To visualize the output of the clustering by feature, each piglet that fell within the control, mild and severe groups was assigned a different shape based on their group, and the output was shown by using a different color for each cluster. This allowed the differentiation of the known group from the assigned cluster (see Figure 5.1).

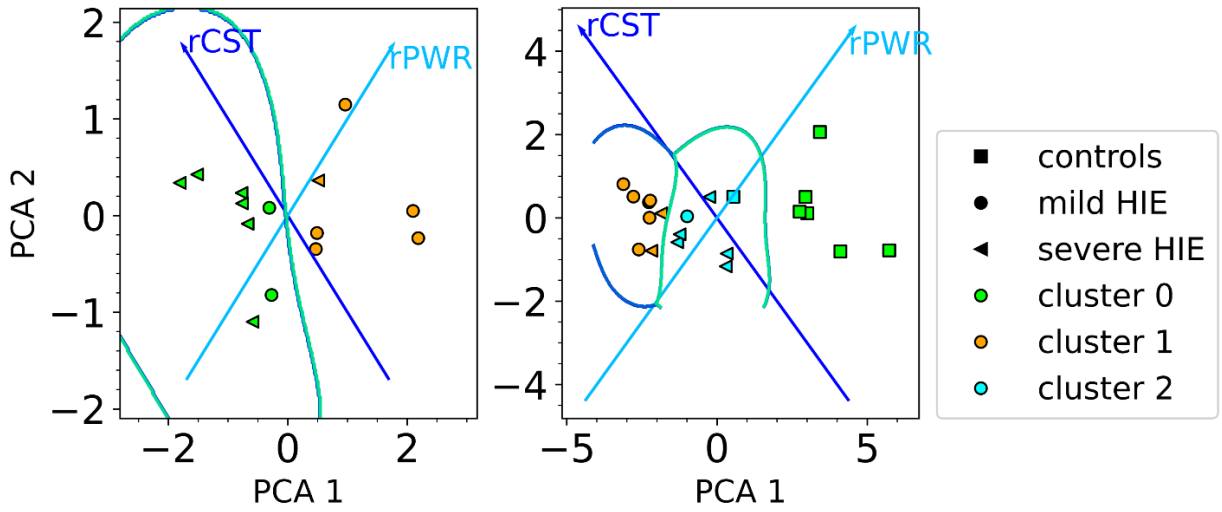


Fig.5.1. The results of the HIE piglet classification, showing the contour by which, the clusters were differentiated. The feature shown is the area under the curve normalized by the duration of the insult.

In Fig.5.1, the Area Under the Curve, post normalization by insult duration, is shown to be a feature that when passed through the clustering pipeline that was developed, can reveal groupings that match the groups defined by the Lact/NAA ratio-based classification of brain injury severity. This method also enabled the examination of outliers, as they can be identified through their mismatch in classification and initial grouping. Such phenomena were hence identified on a feature-by-feature basis. These outliers were attributed to the fact that the pipeline was tested on the isolated feature basis, which masked phenomena captured by the other features. More specifically, when considering the area under the curve on its own, the physiology captured by features such as the reference value or the peak value reached during the insult are not present. Hence, the discrepancy on this level between piglet groups and identified clusters highlighted the importance of combining features to capture the entire physiology being studied. The parameters of the radial basis function were found

by tuning that applied a grid search algorithm. This allowed the definition of the decision boundary contours, whose parameters are shown in Table II.

Table II

| Parameter | Value |
|---|---|
| γ | 0.7 |
| C | 1 |

Table II. A table detailing the values of the radial basis function parameters.

The parameters found provided an indication of the elasticity of the boundaries; however, it was the output of the clustering that was used as the classification of the piglets. Despite this, as shown in Fig.5.1, the tuned radial basis function was able to capture the separate clusters, indicated with different colors, both in the 2-group case, as well as in the 3-group case where controls were also present in the dataset.

Applying the pipeline to the two datasets, namely of z space and *rpwr-rcst* space, for each feature, allowed the quantification of the accuracy of the method for each biomarker in the signal and revealed the importance of insults pertaining to the injury to the pipeline. This was seen more clearly by comparing the rand index score generated for each case.

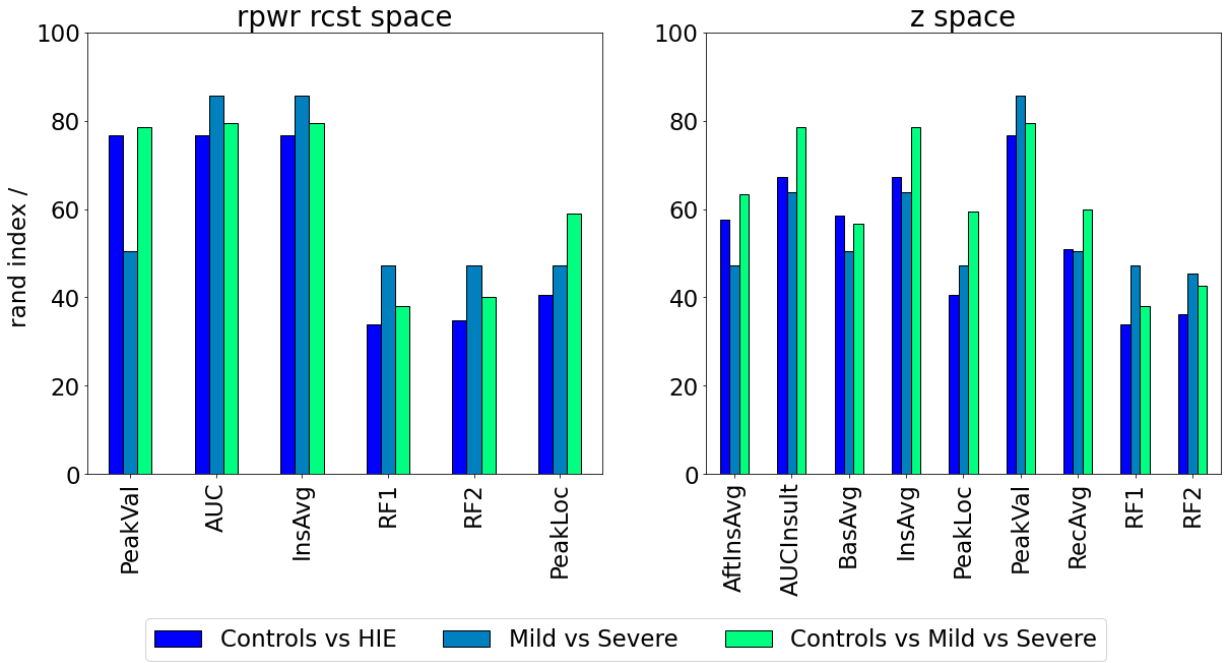


Fig.5.2. The accuracy of clustering using data in z-space and the accuracy of clustering using the relative power and relative cost. The two datasets were not combined to minimize the inter-correlation between quantities. RF1 and RF2 correspond to frequency channels from the 2 instruments in the optical configuration used.

It was shown that it was possible to identify all 3 scenarios successfully. Notably, the area under the curve for the mild vs severe case in the *rpwr-rcst* space reached an accuracy of 84%. The cases of Controls vs HIE and Controls vs Mild vs Severe exhibited an accuracy consistently above 70%, using the R *rpwr-rcst* features. The average performance of the pipeline using the z-space dataset was higher than the average performance using the relative power relative cost dataset. This can be attributed to the increasing effect of inter-correlations when considering multiple quantities, as the underlying effects can be over-represented in the analysis.

## 6. DISCUSSION

The algorithm identified the groups of brain injury severity. Interestingly, the decision boundary that had been found for 2 groups, between controls and HIE, assumed a similar partitioning with the inclusion of further partitioning of HIE piglets into moderate and severe HIE cases. Hence, despite the increased complexity, the control group was unchanged, and still fully identifiable from the other cases. The results agreed with the grouping that was identified through the consideration of the Lac/NAA score, however there were cases of different features performing better. In no case did the decision boundary span strictly from negative to positive relative power or relative cost, signifying that the underlying processes are a result of the complete interaction between the quantities.

The accuracy for each feature confirmed the hypothesis that some features perform better than others when being deployed in a clustering–based pipeline. The best-performing features when considering the features generated in the z space were the signal average, the value of the peak and the normalised AUC during the insult. Similarly, the relative power space features were dominated in terms of accuracy by the same 3 variables. The advantage of this method was that it also allowed the recognition of non-mutual features as useful, such as the signal average after insult, which did not exist in the relative power space dataset, yet in the z space performed well, further proving that the before and after desaturation event periods can reveal useful clinical information.

It was observed that features that were directly related to the protocol followed did not lead to accuracy as high as the features that were related to the injury. This is attributed to the controlled nature of the experiment, which had vital signals of the piglets be closely monitored and regularized. An example of this is the feature PeakLoc, which defined the location in time at which the hypoxic-ischemic insult was introduced, which was defined by the experimental procedure that was applied.

This work is a steppingstone to create processing pipelines that open the door for optical data to be utilized in new computational techniques. So far, there have been mentions of NIRS being a good candidate for machine learning models[12]. Our study examined the applicability of machine learning by testing the performance of features that can be extracted from the optical signals and putting forward a pipeline with which the combination of AI and optical data processing could be achieved. The power of this method also lies in the data that is being processed. Previous studies with piglet data have shown that near-infrared spectroscopy data can provide significant biomarkers of HI injury[13].

Previous work in this piglet model of neonatal encephalopathy exhibited the relationship of oxCCO and tissue oxygenation with outcome[14]. The piglet model developed pointed to the presence of clinically important mechanisms that manifest before the HI insult[15]. The underlying mechanisms were indirectly observed through this work, by the examination of the correlations between the features and the identification of outliers when treating each feature separately. That way the missing mechanisms were probed as missing pieces in the pipeline.

## 7. CONCLUSION

In this paper we developed a Machine Learning methodology to integrate bNIRS and DCS measured physiological information of brain oxygenation, haemodynamics, blood flow and metabolism. We demonstrated that the proposed algorithm is able to identify groups of HI brain injury severity in a cohort of piglets with 84% accuracy. Moreover, the pipeline was successful in identifying 3 groups of piglets, namely controls, piglets with mild insult and piglets with severe insult. The developed algorithm also classified piglets that were controls and piglets which had an induced HI insult.

The processing of each feature independently highlighted that the area under the curve, the peak value and the insult average consistently provided clusters that were sensitive to the piglet groups. This was attributed to the fact that the afore-mentioned features reflected changes in the physiology of the piglet before, during and after the insult. In contrast, features that were attributes of the protocol, such as the time at which the insult was induced, yielded a performance in clustering that corresponded to a classification using a random guess. We also showed that the performance of the algorithm in the *rpwr – rcst* space was comparable to the performance of the algorithm when applied to features in the z space, provided that the features corresponded to the physiology of the piglets. This highlighted the importance of taking into consideration the underlying system dependencies, by considering the coupling between the multimodal measurements that were part of the study.

This work included limitations that resulted from the small sample size not only of the total population used, but also of the few samples that were in each group. Moreover, the consideration of each feature separately led to the masking of phenomena that comprised the complete physiology of the piglet during the insult. Future work in this area could focus on the consideration of a larger sample size, and test different clustering techniques. To aid the explanation of the results, further dependency tests could be performed. A neuromonitoring platform that combines bNIRS and DCS in combination with a machine learning approach can offer an innovative solution to identify brain injury. We are currently investigating the use of this approach in the neonatal intensive care unit.

## REFERENCES


[1] Allen, K. A., Brandon, D. H., "Hypoxic ischemic encephalopathy: Pathophysiology and experimental treatments," Newborn and Infant Nursing Reviews 11(3), 125–133 (2011).

[2] Chavez-Valdez, R., Miller, S., Spahic, H., Vaidya, D., Parkinson, C., Dietrick, B., Brooks, S., Gerner, G. J., Tekes, A., et al., "Therapeutic hypothermia modulates the relationships between indicators of severity of neonatal hypoxic ischemic encephalopathy and serum biomarkers," Frontiers in Neurology 12 (2021).

[3] Mitra S, Kendall GS, Bainbridge A, Sokolska M, Dinan M, Uria-Avellanal C, Price D, Mckinnon K, Gunny R, Huertas-Ceballos A, Golay X, Robertson NJ. Proton magnetic resonance spectroscopy lactate/N-acetylaspartate within 2 weeks of birth accurately predicts 2-year motor, cognitive and language outcomes in neonatal encephalopathy after therapeutic hypothermia. Arch Dis Child Fetal Neonatal Ed. 2019 Jul;104(4):F424-F432.

[4] Wang, J., Guan, C., Chen, J., Dou, K., Tang, Y., Yang, W., Shi, Y., Hu, F., Song, L., et al., "Validation of bifurcation definition criteria and comparison of stenting strategies in true left main bifurcation lesions," Scientific Reports 10(1) (2020).

[5] Aliefendioğlu, D., Doğru, T., Albayrak, M., DibekMısırlıoğlu, E., Şanlı, C., "Heart rate variability in neonates with hypoxic ischemic encephalopathy," The Indian Journal of Pediatrics 79(11), 1468–1472 (2012).

[6] Harvey-Jones, K., Lange, F., Tachtsidis, I., Robertson, N. J., Mitra, S., "Role of optical neuromonitoring in neonatal encephalopathy—current state and recent advances," Frontiers in Pediatrics 9 (2021).

[7] Bale, G., Rajaram, A., Kewin, M., Morrison, L., Bainbridge, A., Diop, M., St Lawrence, K., Tachtsidis, I., "Broadband nirs cerebral cytochrome-c-oxidase response to anoxia before and after hypoxic-ischaemic injury in piglets," Advances in Experimental Medicine and Biology, 151–156 (2018).

[8] Tachtsidis, I., Tisdall, M. M., Pritchard, C., Leung, T. S., Ghosh, A., Elwell, C. E., Smith, M., "Analysis of the changes in the oxidation of brain tissue cytochrome-c-oxidase in traumatic brain injury patients during hypercapnoea," Oxygen Transport to Tissue XXXII, 9–14 (2011).

[9] Kaynezhad, P., Mitra, S., Bale, G., Bauer, C., Lingam, I., Meehan, C., Avdic-Belltheus, A., Martinello, K. A., Bainbridge, A., et al., "Quantification of the severity of hypoxic-ischemic brain injury in a neonatal preclinical model using measurements of cytochrome-c-oxidase from a miniature broadband-near-infrared spectroscopy system," Neurophotonics 6(04), 1 (2019).

[10] Rajaram, A., Bale, G., Kewin, M., Morrison, L. B., Tachtsidis, I., St. Lawrence, K. and Diop, M., "Simultaneous monitoring of cerebral perfusion and cytochrome c oxidase by combining broadband near-infrared spectroscopy and diffuse correlation spectroscopy," Biomed. Opt. Express 9(6), 2588 (2018).

[11] P. Pinti et al. “An analysis framework for the integration of broadband NIRS and EEG to assess neurovascular and neurometabolic coupling”. In: Scientific Reports 2021 11:1 11 (1 Feb. 2021), pp. 1–20. issn: 2045-2322. doi: 10.1038/s41598- 021- 83420- 9. url: https://www.nature.com/articles/s41598- 021- 83420-9.

[12] Shu Ling Chong et al. “Predictive modeling in pediatric traumatic brain injury using machine learning”. In: BMC Medical Research Methodology 15 (1 2015). issn: 14712288. doi: 10.1186/S12874- 015- 0015-0. url: /pmc/articles/PMC4374377/%20/pmc/articles/PMC4374377/?report=abstract% 20https://www.ncbi.nlm.nih.gov/pmc/articles/PMC4374377/.

[13] Gemma Bale et al. “Investigation of Cerebral Autoregulation in the Newborn Piglet During Anaesthesia and Surgery”. In: Advances in Experimental Medicine and Biology 812 (2014), p. 165. issn: 22148019. doi: 10 . 1007 / 978 - 1 - 4939 - 0620 - 8 _ 22. url: /pmc/articles/PMC4340574/%20/pmc/articles/PMC4340574/?report=abstract%20https: //www.ncbi.nlm.nih.gov/pmc/articles/PMC4340574/.

[14] Harvey-Jones, K., Lange, F., Verma, V. et al. “Early assessment of injury with optical markers in a piglet model of neonatal encephalopathy”. In: Pediatr Res (2023).

[15] Rajaraman G. “Effect of diltiazem isomers and thiamine on piglet liver microsomal peroxidation using dichlorofluorescein”. In: J Pharm Science (2007)